Published in final edited form as:
J Neurosurg Spine. 2009 October ; 11(4): 432–437. doi:10.3171/2009.4.SPINE08784.

Importance of the vasculature in cyst formation after spinal cord injury

Gemma E. Rooney, Ph.D.[1], **Toshiki Endo, M.D., Ph.D.**[1], **Syed Ameenuddin, D.V.M., Ph.D.**[1], **Bingkun Chen, M.D., Ph.D.**[1], **Sandeep Vaishya, M.D.**[1], **LouAnn Gross**[1], **Terry K. Schiefer, M.D.**[1], **Bradford L. Currier, M.D.**[2], **Robert J. Spinner, M.D.**[3], **Michael J. Yaszemski, M.D., Ph.D.**[2], and **Anthony J. Windebank, M.D.**[1]

[1] Department of Neurology and Molecular Neuroscience, Mayo Clinic College of Medicine, Rochester, Minnesota

[2] Department of Orthopedic Surgery and Bioengineering, Mayo Clinic College of Medicine, Rochester, Minnesota

[3] Department of Neurologic Surgery, Mayo Clinic College of Medicine, Rochester, Minnesota

Abstract

Object—Glial scar and cystic formation greatly contribute to the inhibition of axonal regeneration after spinal cord injury (SCI). Attempts to promote axonal regeneration are extremely challenging in this type of hostile environment. The objective of this study was to examine the surgical methods that may be used to assess the factors that influence the level of scar and cystic formation in SCI.

Methods—In the first part of this study, a complete transection was performed at vertebral level T9–10 in adult female Sprague-Dawley rats. The dura mater was either left open (control group) or was closed using sutures or hyaluronic acid. In the second part of the study, complete or subpial transection was performed, with the same dural closure technique applied to both groups. Histological analysis of longitudinal sections of the spinal cord was performed, and the percentage of scar and cyst formation was determined.

Results—Dural closure using sutures resulted in significantly less glial scar formation ($p = 0.0248$), while incorporation of the subpial transection surgical technique was then shown to significantly decrease cyst formation ($p < 0.0001$).

Conclusions—In this study, the authors demonstrated the importance of the vasculature in cyst formation after spinal cord trauma and confirmed the importance of dural closure in reducing glial scar formation.

Keywords

traumatic spinal cord injury; vascular injury; glial cell response to injury

For an experimental model of SCI to be effective it must produce consistent injuries, which should be clinically relevant in terms of functional and histopathological outcomes. Current

Address correspondence to: Anthony J. Windebank, M.D., Mayo Clinic College of Medicine, 15 Guggenheim Building, 200 First Street SW, Rochester, Minnesota 55905. windebank.anthony@mayo.edu.

Disclosure

Funding for this work was provided by the Mayo Foundation and the Craig Neilsen Foundation. Dr. Windebank received support from the National Institute of Biomedical Imaging and BioEngineering of the NIH, grant number EB02390.

This article contains some figures that are displayed in color online but in black and white in the print edition.

animal models of SCI include contusion, compression, and transection injuries. Contusion models represent the type of injury that occurs most often in patients.[10] Spinal cord contusion causes extensive damage to motor neurons and roots over several spinal cord segments, leading to the induction of large cysts and scar formation. Complete transection models enable separate manipulation of the pial and dural coverings, which facilitates study of how the vasculature contributes to the SCI pathology.

During the acute phase of SCI, hemorrhage around the injury site occurs, which leads to a disruption in oxygen and nutrient supply to all cells in the area. An inflammatory immune response ensues, with infiltration of neutrophils to the site of injury. This inflammatory response, combined with vascular damage, results in edema after the insult.[6,7] Formation of a glial scar occurs during the secondary phase of SCI. The glial scar consists of reactive astrocytes, microglia, fibroblasts, and schwann cells,[14] and has been identified as a major inhibitory factor to neuronal regeneration after traumatic injury to the CNS.[17] Often fluid-filled cysts can form centrally at the site of injury, which progressively expand, and further contribute to cell death and axonal inhibition.[6] The reason for the formation of such cysts is unknown.

Innovative microsurgical techniques may be used to reduce hemorrhaging, gliosis, and cavitation after transection SCI,[19] thereby optimizing the potential for axonal regeneration at the injury site. Seitz et al.[12] demonstrated functional recovery after complete transection of the spinal cord in mice without any cellular or molecular intervention. These authors attributed return of function to minimal dural injury, minimal displacement of spinal cord stumps, and minimal fibroblastic infiltration. In a dorsal hemisection model of SCI, reduced lesion gap, cystic cavitation, and connective tissue scar formation occurred as a result of dural closure.[18] Application of a potent iron chelator and cyclic adenosine monophosphate was shown to reduce fibrous scarring, thereby promoting long distance corticospinal tract regeneration in rats that received a dorsal corticospinal tract transection.[9]

In this study we examined the surgical methods that may be used to reduce the level of scar and cystic formation in complete transection SCI models. Our main objective was to assess the extent to which disruption of the vasculature influenced scar and cyst formation after SCI.

Methods

Complete Transection and Dural Closure Surgeries

All procedures involving animals were approved by the Institutional Animal Care and Use Committee at the Mayo Clinic. Adult female Sprague-Dawley rats (250–300 g) were anesthetized with 80 mg/kg ketamine (Fort Dodge Animal Health) and 5 mg/kg xylazine (Ben Venue Laboratories) via intraperitoneal injection. Akwa Tears lubricant opthalamic ointment (Akron, Inc.) was used to prevent drying of the eyes during surgery.

Hair was clipped from each animal's back, and the site of incision was disinfected using Povidone-Iodine Scrub Swabsticks (Professional Disposables, Inc.). The heating pad temperature was constantly maintained at 37°C during surgery. The operation was performed using a sterile technique with the aid of a Zeiss OPMI-6 surgical microscope. A 2-cm midline incision was made along the T-7 to T-10 spinous processes. The thoracolumbar fascia and paraspinal musculature were incised along the spinous processes and retracted. A laminectomy was performed at the level of T9–10. The dura mater was incised 5 mm longitudinally using a microforceps and micro scissors. Hemostasis was obtained with the application of light pressure with a cotton swab until the bleeding stopped. The spinal cord was then cut transversely using a microsurgical knife. The completeness of the transection was confirmed by passing a microhook between the 2 cut ends. The muscles, subcutaneous tissue, and skin were sutured closed in 1 group of 11 animals, while in the other 2 groups, the dura was also

closed by either a running 10–0 prolene suture in 12 rats, or using a topical 0.1-ml high molecular weight hyaluronic acid gel (Daltons, Healon; Pharmacia) in 4 rats. The completeness of dural closure was confirmed by observing CSF filling the subdural space, none of which leaked through the closed dura.

Subpial Transection Surgeries

In the second part of this study, we sought to compare the effects of complete and subpial transection on glial scar and cyst formation. In 1 group of animals (9 rats) complete transection followed by dural closure using sutures was performed as described above. In the second group of animals (8 rats), subpial transections were performed. A laminectomy was performed and the spinal cord was approached from a lateral orientation. Under direct observation of the dorsal vein, a microsurgical knife was placed horizontally just beneath the vein and directed all the way to the other side. The knife was then rotated, cutting the spinal cord in a single turn, keeping the dorsal spinal vasculature (both arterial supply and venous drainage) intact (Fig. 1). The dura was also closed with sutures.

Postoperative Care

Postoperatively, animals were given buprenorphine 0.05 mg/kg subcutaneously for pain for the first 48 hours, Lactated Ringer's solution was administered as needed, and gentamycin was given (Schering-Plough) intramuscularly for 3–7 days to prevent infection. For the duration of the experiment, bladder voiding and observation of the animals was performed twice daily. Topical antibiotic ointments were used to treat decubital ulcers.

Spinal Cord Tissue Harvesting

Animals from the dural closure study were killed 1-month postsurgery, while those from the subpial transection study were killed 2 hours and 3 weeks postsurgery. All animals were killed with intramuscular injections of pentobarbital (Fort Dodge Animal Health), and fixation was performed by transcardial perfusion with 4% paraformaldehyde. The spinal columns were removed en bloc and postfixed in 4% paraformaldehyde for 48 hours. The spinal cords (including the transected area plus 1 cm above and below the lesion) were then removed and postfixed in 4% paraformaldehyde for an additional 24–48 hours before being embedded in paraffin, and 8-μm longitudinal serial sections were taken. The longitudinal sections were oriented in the sagittal plane. Throughout the entire sagittal spinal cord, 12-to-15 × 8–μm sections were collected for analysis at 150-μm intervals. Complete transection of the spinal cord was observed in every case. Sectioning was performed using a Reichert Jung tabletop microtome.

Histological Analysis

Masson trichrome staining was performed on tissue sections obtained from all animal groups. Briefly, sections were washed in tap water and then stained with hematoxylin for 10 minutes. After rinsing, sections were stained with Biebrich scarlet for 5 minutes, rinsed, and placed in phosphotungstic/phosphomolybdic acid for 10 minutes. Sections were then transferred directly into Aniline blue for 5 minutes, rinsed, and placed in 1% acetic acid for 1 minute. After rinsing, the sections were dehydrated, cleared, and coverslipped. All reagents were from Sigma-Aldrich.

Image acquisition was performed using a Zeiss AxioCam loaded on a Zeiss Axio Imager Z1 microscope, and Zeiss KS400 software was used to determine the percentage normal cord, scar formation, and cyst formation. These areas are outlined in Fig. 2. The thick black line delineates the area within which the measurements were taken. This area excluded scarring extrinsic to the spinal cord. Cysts were identified as fluid-filled cavities (surrounded by thin black lines),

while scar was identified as spinal cord tissue infiltrated with collagen (blue tissue), because collagen is not normally found in the spinal cord. The normal spinal cord is delineated by a thin red line. All analyses were carried out by blinded observers.

Statistical Analysis

The 1-way ANOVA was used, with post-hoc analysis performed using the Bonferroni test for the first dural closure study. The Student unpaired t-test was used to analyze the subpial transection data. Values of $p \leq 0.05$ were considered statistically significant. Commercially available software (Graph Pad Prism 4) was used for all analyses.

Results

Dural Closure

A mortality rate of ~ 20% was observed in these transection studies. Masson trichrome staining was used to identify collagen-rich areas. Figure 3 distinguishes collagenous areas (in blue) from the cytoplasm (in red). Collagen staining appeared to be more extensive in animals that had their dura left open (9 rats analyzed; Fig. 3A and B) compared with those that had their dura closed with sutures (7 rats analyzed) or hylaluronic acid (4 analyzed; Fig. 3C–F). This was confirmed by morphometric analysis of the area of glial scar in the different groups (Fig. 4). Animals in which the dura was sutured closed demonstrated significantly less scar formation compared with all other groups ($p = 0.0248$). Hyaluronic acid closure showed a trend toward reduced glial scar formation, but this did not reach statistical significance. Dural closure did not, however, have any significant impact on the extent of cyst formation.

The entire spinal cord was sectioned longitudinally and was sampled at 150-μm intervals. This confirmed that all groups did indeed receive a complete transection injury.

Subpial Transection

As with the complete transection injury (8 rats analyzed), the spinal cord was exposed at vertebral level T9–10 (Fig. 5A) for the subpial transection (in 7 rats). The spinal cord was then transected without disrupting the vasculature (Fig. 5B), and the dura above the transected site was sutured closed (Fig. 5C).

Trichrome staining performed 2 hours postsurgery confirmed that the spinal cord was completely transected and demonstrated that in general the distance between the spinal cord stumps in the complete transection injury (Fig. 6A) was greater than in the subpial transection injury (Fig. 6B); this was not directly measured, however. Trichrome staining 3 weeks postsurgery showed excessive infiltration of collagenous tissue and larger cystic spaces in the complete transected cord (Fig. 6C and E) compared with the subpially transected cord (Fig. 6D and F).

These findings were confirmed by morphometric analysis of the area of cystic formation between the 2 groups (Fig. 7). A similar reduction in scar formation after dural closure in our first study (Fig. 4) was noted. In both groups, we performed a complete transection with dural closure. In the subpial group, in which the pial vasculature was preserved, there was an additional significant decrease in cyst formation compared with rats with complete transection with dural closure ($p < 0.0001$). This, in turn, resulted in a significantly greater percentage of normal spinal cords ($p = 0.049$).

Discussion

Complete transection SCI models provide an excellent platform for assessing how therapeutic strategies impact axonal regeneration without the confounding factor of sprouting from surviving axons. Furthermore, transection injuries allow for the delivery of various cell types (such as schwann cells and neural stem cells) and trophic factors via biodegradable scaffolds,[1,3,4,8,11,13,15,16] thereby providing a structural framework on which regeneration can take place. Formation of glial scars and cystic cavities contribute to the inhibition of axonal regeneration after a spinal cord trauma[6,14] and can be quite extensive in transection SCI models. Our objective was to determine the effect of the vasculature on scar and cyst formation after a transection SCI.

Importance of Dural Closure

Failure to repair the dura mater after spinal cord trauma can lead to the formation of a more extensive glial scar because of infiltration by meningeal cells coupled with ingrowth of connective tissue from the surrounding soft tissue and muscle.[2,5] Suturing of the dura in the event of a dorsal hemisection has been shown to reduce lesion gap, cystic cavitation, and connective tissue scar formation. [18] We found a significant decrease in scar formation resulting from dural closure in the complete transection model. Collagen is a very suitable marker for the anatomical scar. Chondroitin sulfate proteoglycans may be used to delineate the so-called molecular scar, while glial fibrillary acidic protein is a good marker for the cellular reaction in the spinal cord. Unlike collagen, however, these markers may not necessarily correlate with the anatomical scar.

A novel hyaluronic acid closure technique was used in this study and compared with dural suturing. Although the use of hyaluronic acid also showed a trend toward a reduction in the percentage scar formation, this effect was not statistically significant. Dural closure with sutures did result in significantly less glial scarring, thereby confirming previous reports of extensive scar formation resulting from infiltrating cells traversing a compromised dura.[2,5] Cyst formation and observation of lesion gap size between spinal stumps remained unaffected by dural closure, however. In the present study we were able to confirm dural closure at the time of surgery but cannot exclude the possibility of subsequent leakage.

Role of Pial Vascular Preservation

The failure to reduce the lesion size between spinal stumps and the formation of cystic cavities prompted us to take the transection model further. We endeavored to induce a subpial complete transection of the spinal cord without disrupting the overlying vasculature, and coupled this technique with the dural closure procedure. This resulted in a similar reduction in glial scar formation comparable to complete transection with dural closure. However, implementation of this technique was also accompanied by a significant decrease in the formation of cystic cavities as demonstrated on histological and morphometric analyses. We could therefore conclude that destruction of the overlying vasculature significantly contributes to cyst formation in SCI, which in turn leads to secondary cell death. Examination of spinal cords 2 hours posttransection also revealed a reduction in the gap size between spinal stumps in animals that underwent subpial transection, an observation that was not directly quantified. Maintenance of the vasculature therefore facilitates apposition of spinal stumps in transection injuries.

Conclusions

In the present study we have demonstrated the importance of the vasculature in cyst formation after a spinal cord trauma and confirmed the importance of dural closure in reducing glial scar

formation. We have also presented an evolved transection model (subpial transection coupled with dural closure) that may now provide an ideal platform for the study of various molecular and cellular approaches to axonal regeneration. Promotion of functional recovery in complete transection injuries will probably require a combination of therapeutic strategies focused on reducing the level of axonal inhibition at the site of injury, and thereby increasing the potential for regeneration of endogenous or transplanted neurons.

Acknowledgments

The authors thank James Tarara from the Optical Morphology Core Facility, for his assistance, and David Factor from Illustration and Design for creating the schematic images in Fig. 1.

Abbreviation used in this paper

SCI spinal cord injury

References

1. Bunge MB. Bridging the transected or contused adult rat spinal cord with Schwann cell and olfactory ensheathing glia transplants. Prog Brain Res 2002;137:275–282. [PubMed: 12440373]
2. Fernandez E, Pallini R. Connective tissue scarring in experimental spinal cord lesions: significance of dural continuity and role of epidural tissues. Acta Neurochir (Wien) 1985;76:145–148. [PubMed: 4025022]
3. Friedman JA, Lewellyn EB, Moore MJ, Schermerhorn TC, Knight AM, Currier BL, et al. Synthes Award for Resident Research in Spinal Cord & Spinal Column Injury: Surgical repair of the injured spinal cord using biodegradable polymer implants to facilitate axon regeneration. Clin Neurosurg 2004;51:314–319. [PubMed: 15571160]
4. Friedman JA, Windebank AJ, Moore MJ, Spinner RJ, Currier BL, Yaszemski MJ. Biodegradable polymer grafts for surgical repair of the injured spinal cord. Neurosurgery 2002;51:742–752. [PubMed: 12188954]
5. Frisen J, Risling M, Korhonen L, Zirrgiebel U, Johansson CB, Cullheim S, et al. Nerve growth factor induces process formation in meningeal cells: implications for scar formation in the injured CNS. J Neurosci 1998;18:5714–5722. [PubMed: 9671662]
6. Hagg T, Oudega M. Degenerative and spontaneous regenerative processes after spinal cord injury. J Neurotrauma 2006;23:264–280. [PubMed: 16629615]
7. Hulsebosch CE. Recent advances in pathophysiology and treatment of spinal cord injury. Adv Physiol Educ 2002;26:238–255. [PubMed: 12443996]
8. Jin Y, Fischer I, Tessler A, Houle JD. Transplants of fibroblasts genetically modified to express BDNF promote axonal regeneration from supraspinal neurons following chronic spinal cord injury. Exp Neurol 2002;177:265–275. [PubMed: 12429228]
9. Klapka N, Hermanns S, Straten G, Masanneck C, Duis S, Hamers FP, et al. Suppression of fibrous scarring in spinal cord injury of rat promotes long-distance regeneration of corticospinal tract axons, rescue of primary motoneurons in somatosensory cortex and significant functional recovery. Eur J Neurosci 2005;22:3047–3058. [PubMed: 16367771]
10. Kwon BK, Oxland TR, Tetzlaff W. Animal models used in spinal cord regeneration research. Spine 2002;27:1504–1510. [PubMed: 12131708]
11. Moore MJ, Friedman JA, Lewellyn EB, Mantila SM, Krych AJ, Ameenuddin S, et al. Multiple-channel scaffolds to promote spinal cord axon regeneration. Biomaterials 2006;27:419–429. [PubMed: 16137759]
12. Seitz A, Aglow E, Heber-Katz E. Recovery from spinal cord injury: a new transection model in the C57Bl/6 mouse. J Neurosci Res 2002;67:337–345. [PubMed: 11813238]
13. Teng YD, Lavik EB, Qu X, Park KI, Ourednik J, Zurakowski D, et al. Functional recovery following traumatic spinal cord injury mediated by a unique polymer scaffold seeded with neural stem cells. Proc Natl Acad Sci U S A 2002;99:3024–3029. [PubMed: 11867737]

14. Thuret S, Moon LD, Gage FH. Therapeutic interventions after spinal cord injury. Nat Rev Neurosci 2006;7:628–643. [PubMed: 16858391]

15. Xu XM, Guénard V, Kleitman N, Bunge M. Axonal regeneration into Schwann cell-seeded guidance channels grafted into transected adult rat spinal cord. J Comp Neurol 1995;351:145–160. [PubMed: 7896937]

16. Xu XM, Zhang SX, Li H, Aebischer P, Bunge MB. Regrowth of axons into the distal spinal cord through a Schwann-cell-seeded mini-channel implanted into hemisected adult rat spinal cord. Eur J Neurosci 1999;11:1723–1740. [PubMed: 10215926]

17. Yiu G, He Z. Glial inhibition of CNS axon regeneration. Nat Rev Neurosci 2006;7:617–627. [PubMed: 16858390]

18. Zhang YP, Iannotti C, Shields LB, Han Y, Burke DA, Xu XM, et al. Dural closure, cord approximation, and clot removal: enhancement of tissue sparing in a novel laceration spinal cord injury model. J Neurosurg 2004;100:343–352. [PubMed: 15070142]

19. Zingale A. An experimental model to study axonal regeneration of the rat spinal cord*. J Neurosurg Sci 1989;33:329–331. [PubMed: 2634091]

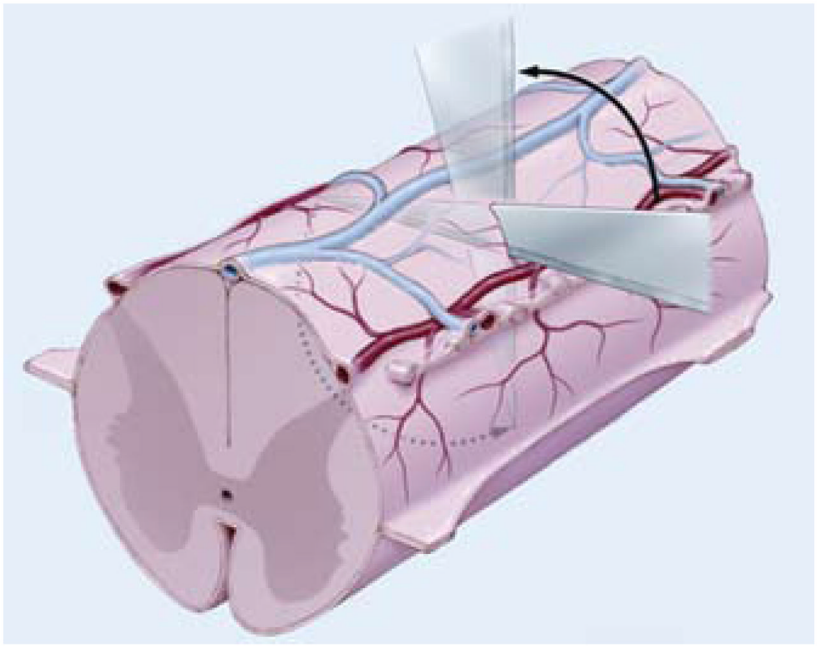

Fig. 1.

Artist's schematic representation of subpial surgical transection technique. Under direct observation of the dorsal vein, a microsurgical knife is placed horizontally just beneath the vein and directed all the way to the other side. The knife is rotated, cutting the spinal cord in one turn while keeping the dorsal spinal vasculature intact.

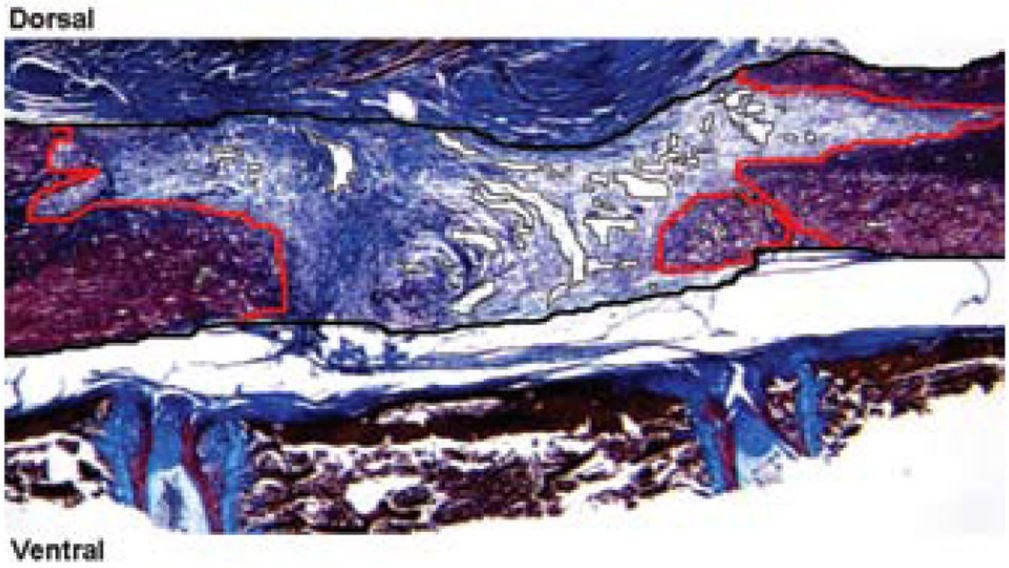

Fig. 2.

Photomicrograph showing a representation of technique used for determining the percentage normal cord, scar formation, and cyst formation on trichrome-stained spinal cord sections. Zeiss KS400 software was used to determine the volume of the spinal cord occupied by cysts, scar or normal spinal cord tissue. The *thick black line* delineates the area within which measurements were taken. Cysts were identified as fluid-filled cavities (surrounded by *thin black lines*), while scar was identified as spinal cord tissue infiltrated with collagen (blue tissue). Normal spinal cord tissue is delineated by a *thin red line*. Original magnification × 25.

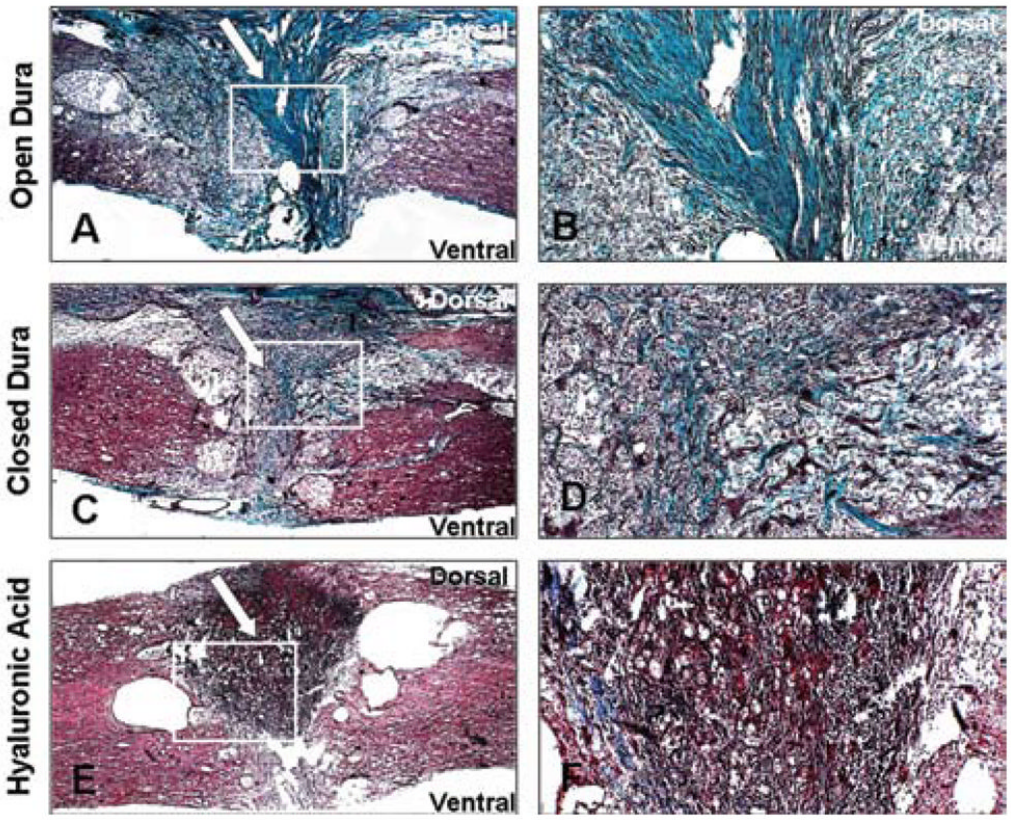

Fig. 3.

Photomicrographs showing histological analysis of the transected spinal cord samples. Trichrome staining of collagen fibers was used in the transected cord where the dura was left open (A and B), sutured closed (C and D), or closed with hyaluronic acid (E and F). *White arrows* indicate collagenous scar tissue areas around the transected cord. *White boxes* denote area where higher magnification images were taken. Magnification: × 25 (A, C, and E); × 100 (B, D, and F).

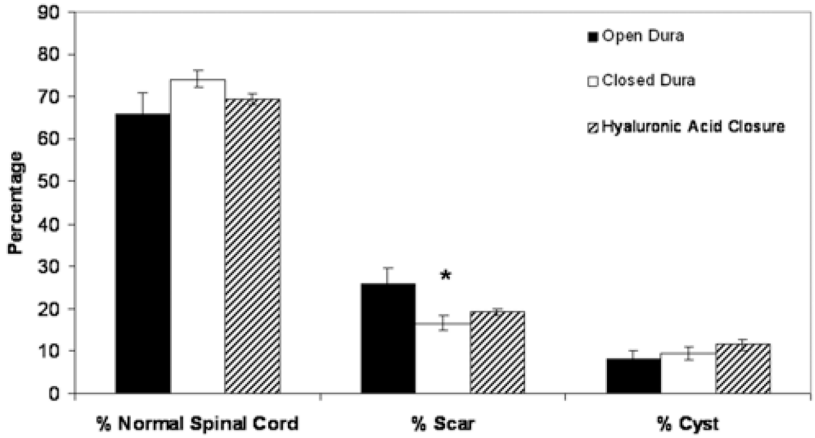

Fig. 4.

Bar graph showing the percentage of normal cord, scar formation, and cystic formation in animals that underwent transection injury without dural closure, or with dural closure using sutures or hyaluronic acid. *Error bars* represent standard error of the mean; *p = 0.0001.

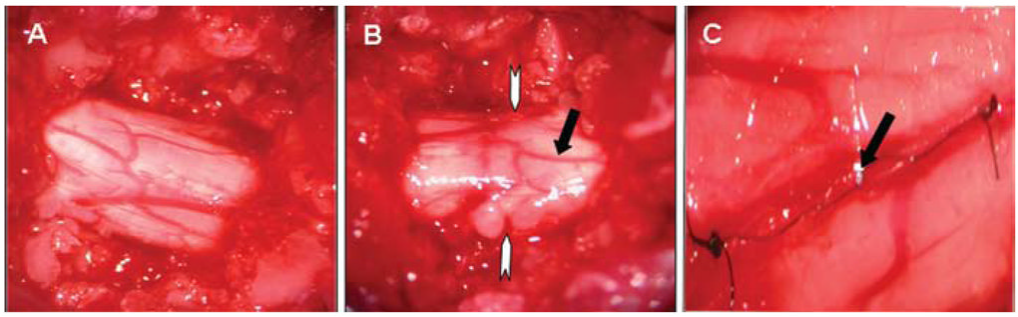

Fig. 5.

Photographs showing the gross anatomy of the rat spinal cord. A: Exposed spinal cord at vertebral level T-9. B: Subpial transection. *White arrows* denote level of transection. *Black arrow* shows the intact dural vasculature with minimal hemorrhage. C: Dural closure with 10–0 sutures. *Black arrow* shows dural suture.

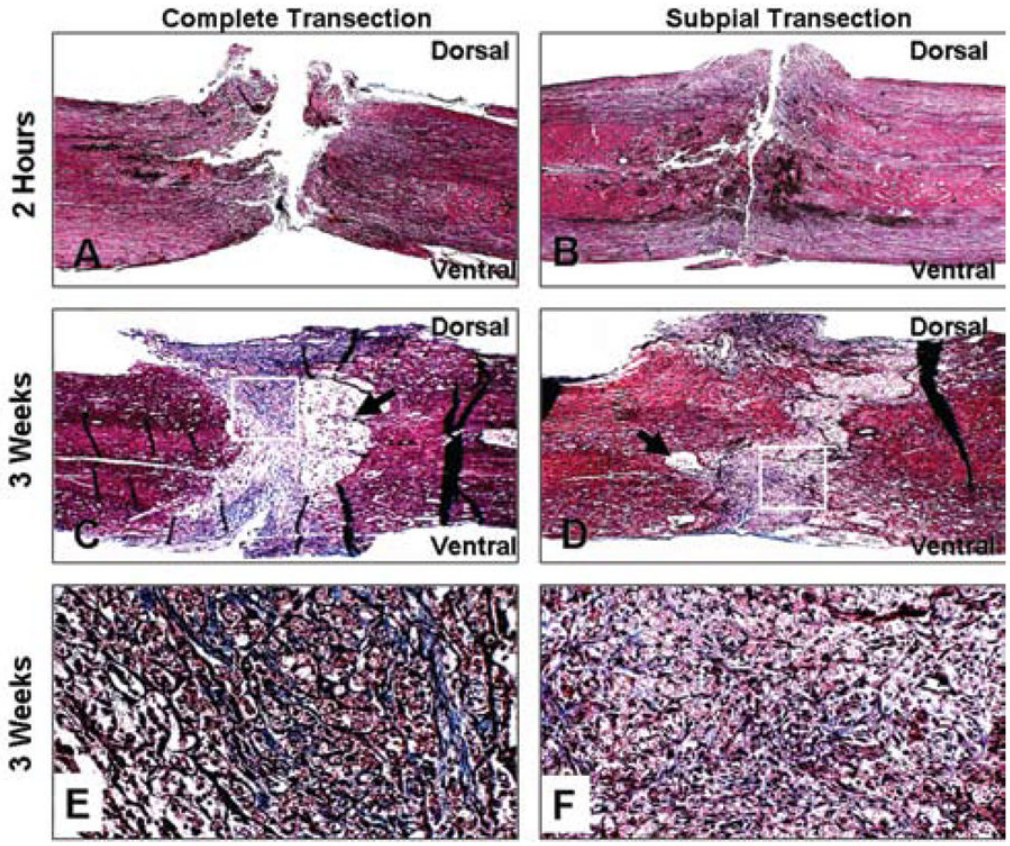

Fig. 6.

Photomicrographs showing histological analysis of complete versus subpial transected spinal cords. Trichrome staining of collagen fibers in the complete transected (A, C, and E) versus subpial transected (B, D, and F) cord 2 hours (A and B) and 3 weeks after surgery (C–F). *Black arrows* in C and D indicate cystic areas. *White boxes* denote area where higher magnification images were taken. Magnification × 25 (A–D); × 200 (E and F).

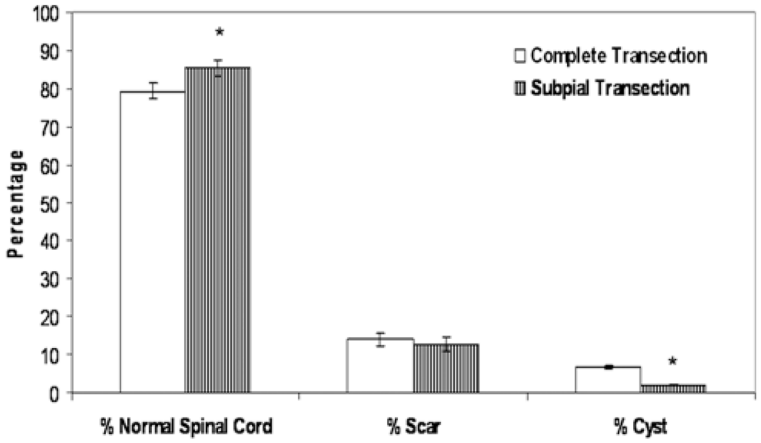

Fig. 7.

Bar graph showing the percentage of normal cord, scar formation, and cystic formation in animals that received complete or subpial transection SCIs. *Error bars* represent SEMs; *$p < 0.05$.